

Four Complexes of Mn(II), Co(II), Ni(II) and Cu(II) Based on 2-Morpholine-4-yl-4,6-di-pyrazol-1-yl-1,3,5-triazine

TIAN Wen-Yu CHU Jin-Feng^①

(State Key Laboratory of Chemical Resource Engineering,
Beijing University of Chemical Technology, Beijing 100029, China)

ABSTRACT Three azide bridged complexes, namely, $[\text{Mn}_2\text{L}_2(\text{N}_3)_4(\text{H}_2\text{O})_2]$ (**1**), $[\text{Co}_2\text{L}_2(\text{N}_3)_4](\text{H}_2\text{O})_3$ (**2**) and $[\text{Ni}_2\text{L}_2(\text{N}_3)_3(\text{H}_2\text{O})]\text{N}_3(\text{H}_2\text{O})_4$ (**3**) ($\text{L} = 2\text{-morpholine-4-yl-4,6-di-pyrazol-1-yl-1,3,5-triazine}$), were synthesized by the reaction of L ligand, sodium azide with Mn(II), Co(II) and Ni(II) chlorides. The copper(II) chloride combined with thiocyanate and L ligand to form a mononuclear complex $[\text{CuL}(\text{CH}_3\text{OH})(\text{SCN})(\text{NCS})]$ (**4**). Complexes **1**~**4** were characterized by IR, elemental analysis and X-ray crystallographic analysis. It was worth noting that two Mn(II) atoms were connected by the end-to-end mode in **1**, while Co(II) and Ni(II) atoms were connected by the end-on mode in **2** and **3**. In complex **4**, the central copper atom was coordinated with a sulfur atom and a nitrogen atom of the two thiocyanate ligands, respectively. Hydrogen bonds, π - π stacking interactions, thermogravimetric analysis and fluorescence properties of **1**~**4** were studied.

Keywords: azide bridged complexes, supramolecular, crystal structure, thiocyanate;

DOI: 10.14102/j.cnki.0254-5861.2011-3033

1 INTRODUCTION

Metal coordination complexes have broad application prospects in the fields of chemistry, biology and medicine^[1]. In recent years, great efforts have been devoted to the rational design and synthesis of new coordination complexes, resulting in fascinating structures and novel applications such as catalysis^[2], optoelectronic devices^[3], energy storage^[4], adsorption^[5], magnetic materials^[6, 7] and so on. As we all know, *s*-triazine ring is a symmetric nitrogen-containing heterocyclic ring, and nitrogen atoms are evenly distributed on the benzene ring. Combined with the introduction of other nitrogen-containing heterocycles, a coordination pattern from monodentate to multidentate can be formed to assemble structure-rich complexes. They play a vital role in energetic materials^[8], multi-functional spin-crossover complexes^[9], supramolecular materials^[10], etc.

Azide anion is a common bridging ligand, which can provide different coordination modes and reflect the versatility of azide ligand^[11]. Depending on the space and electronic requirements of other ligands in the complex, the azide can form bridges in end-to-end ($\mu_{1,3}\text{-N}_3$, EE) and

end-on ($\mu_{1,1}\text{-N}_3$, EO) modes^[12]. The literatures have reported the synthesis of azide multinuclear complexes of Ni(II)^[13], Cu(II)^[14], Mn(II, III)^[15], Co(II, III)^[16] and other metals.

Noncovalent interactions including π - π stacking and hydrogen bonds play important roles in the construction of different supramolecular structures. In our previous study, we synthesized 2-morpholine-4-yl-4,6-di-pyrazol-1-yl-1,3,5-triazine (**L**) ligand, and studied its reactivity with transitional metals and structures of a series of copper(II) and nickel(II) complexes of this ligand^[17-19]. When we further study the supramolecular complexes of L ligand, three azide bridged binuclear complexes with Mn(II), Co(II) and Ni(II) ions were obtained. In addition, when using SCN^- instead of N_3^- , a mononuclear copper(II) complex was prepared.

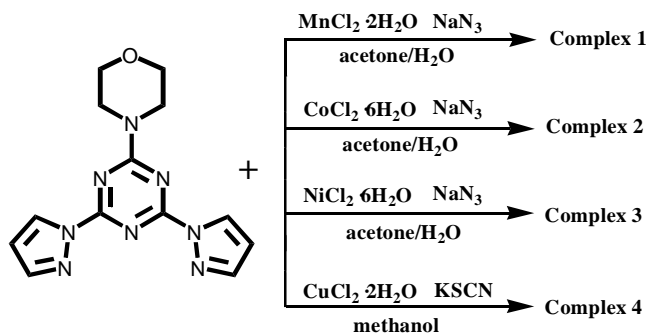
2 EXPERIMENTAL

2.1 Materials and methods

All raw materials and solvents were purchased from Alfa-Aesar. The ligand L was prepared according to the literature^[18]. The synthetic routes of complexes **1**~**4** are shown in Scheme 1. C, H and N analyses were performed

using Perkin-Elmer 2400-II CHN analyzer. A Bruker Vector 22 infrared spectrometer was used to record FT-IR spectra

from KBr particles. The emission spectra were measured with FLS 980 Edinburgh Analyzer.



Scheme 1. Synthetic routes of complexes 1~4

2.2 Synthesis of 1

L ligand (80 mg, 0.27 mmol) and $\text{MnCl}_2 \cdot 2\text{H}_2\text{O}$ (52.8 mg, 0.27 mmol), dissolved respectively in 5 and 15 mL of acetone, were mixed with 4 mL water solution of NaN_3 (104.5 mg, 1.61 mmol). The mixed solution was stirred at room temperature overnight and filtered to obtain an orange solution. After standing for about 3 days, light yellow crystals suitable for X-ray diffraction were obtained from the filtrate. Yield: 31.8 mg, 26%. Anal. Calcd. for $\text{C}_{26}\text{H}_{32}\text{Mn}_2\text{N}_{28}\text{O}_4$ ($M_r = 910.68$): C, 34.29; H, 3.54; N, 43.07%. Found: C, 34.02; H, 3.15; N, 42.75%. IR (KBr pellet, cm^{-1}): 3310(w), 3106(w), 2924(w), 2869(w), 2088(s), 2049(s), 1631(s), 1592(s), 1503(s), 1488(s), 1463(s), 1398(s), 1334(w), 1311(w), 1270(m), 1177(w), 1114(m), 1078(w), 1067(w), 1044(m), 1006(m), 962(w), 936(w), 910(w), 854(w), 810(w), 776(m), 644(m), 598(w), 551(w).

2.3 Synthesis of 2

L ligand (80 mg, 0.27 mmol) and $\text{CoCl}_2 \cdot 6\text{H}_2\text{O}$ (63.7 mg, 0.27 mmol) dissolved respectively in 5 and 15 mL of acetone were mixed with 4 mL water solution of NaN_3 (104.5 mg, 1.61 mmol). The mixed solution was stirred at room temperature overnight and filtered to obtain a purple solution. After standing for about 1 day, purple plate crystals suitable for X-ray diffraction were obtained from the filtrate. Yield: 31.3 mg, 25%. Anal. Calcd. for $\text{C}_{26}\text{H}_{34}\text{Co}_2\text{N}_{28}\text{O}_5$ ($M_r = 936.67$): C, 33.34; H, 3.66; N, 41.87%. Found: C, 33.19; H, 3.54; N, 41.86%. IR (KBr pellet, cm^{-1}): 3423(w), 3099(w), 2853(w), 1638(s), 1606(m), 1503(s), 1489(s), 1470(s), 1396(s), 1307(m), 1267(m), 1182(w), 1111(w), 1071(w), 1043(w), 1014(w), 960(m), 938(w), 908(w), 848(w), 809(w), 797(w), 770(w), 638(w), 592(w), 563(w).

2.4 Synthesis of 3

$\text{NiCl}_2 \cdot 6\text{H}_2\text{O}$ (78 mg, 0.27 mmol) and NaN_3 (104.5 mg,

1.61 mmol) dissolved respectively in 4 mL of water were mixed with 20 mL acetone solution of L ligand (80 mg, 0.27 mmol). The mixed solution was filtered to obtain a light green solution. After standing for about 1 day, green bulk crystals suitable for X-ray diffraction were obtained from the filtrate. Yield: 59 mg, 45%. Anal. Calcd. for $\text{C}_{26}\text{H}_{38}\text{N}_{28}\text{Ni}_2\text{O}_7$ ($M_r = 972.20$): C, 32.12; H, 3.94; N, 40.34%. Found: C, 31.96; H, 3.88; N, 40.13%. IR (KBr pellet, cm^{-1}): 3427(w), 3098(w), 2848(w), 2061(s), 1648(s), 1609(s), 1477(vs), 1402(s), 1307(w), 1270(m), 1186(w), 1107(w), 1076(w), 1048(w), 1020(w), 964(m), 910(w), 845(w), 793(m), 778(w), 662(w), 633(w), 593(w), 568(w), 501(w), 475(w).

2.5 Synthesis of 4

L4 (20 mg, 0.067 mmol) and $\text{CuCl}_2 \cdot 2\text{H}_2\text{O}$ (11.4 mg, 0.067 mmol) were dissolved in 3 mL of methanol and then mixed with 2 mL methanol of KSCN (45.7 mg, 0.47 mmol). The resulting solution was filtered to obtain a brown solution. After about 24 hours, red plate-like crystals were obtained. Yield: 10.6 mg, 31%. Anal. Calcd. for $\text{C}_{16}\text{H}_{18}\text{CuN}_{10}\text{O}_2\text{S}_2$ ($M_r = 510.06$): C, 37.68; H, 3.56; N, 27.46%. Found: C, 37.71; H, 3.52; N, 27.13%. IR (KBr pellet, cm^{-1}): 3425(w), 3123(w), 2922(w), 2866(w), 2134(m), 2078(m), 1624(m), 1589(m), 1499(m), 1483(m), 1463(m), 1397(m), 1307(m), 1263(m), 1177(w), 1116(w), 1074(w), 1040(w), 1011(w), 955(m), 934(w), 908(w), 857(w), 802(m), 769(m), 594(w), 556(w).

2.6 Crystal structure determination

The crystal data of four complexes were measured with $\text{MoK}\alpha$ radiation ($\lambda = 0.71073 \text{ \AA}$) at $95 \sim 107 \text{ K}$ on a multi-metal ratio diffractometer. Using OLEX2^[20], the structures were solved by direct methods with SHELXS program^[21] and refined by full-matrix least-squares techniques on F^2 with SHELXL^[22]. All non-hydrogen atoms were anisotropically refined, and the hydrogen atoms

included in calculation are generated into riding modes at the ideal positions. Table 1 summarizes the crystallographic data of the corresponding molecular structures **1**~**4**. In complex **2**, the occupancy rates of O(2) and N(12), O(4) and N(15), O(5) and N(17) are each 50%. A class B warning appears in

the checkcif report of complex **2** due to the disorder of hydrogen atoms between O(2) and O(3) atoms and the failure to lock their positions. In complex **3**, the occupancy rates of O(2), O(4), O(5) and N(12)~N(17) are each 50%.

Table 1. Crystallographic Data for Complexes **1**~**4**

	1	2	3	4
Formula	C ₂₆ H ₃₂ Mn ₂ N ₂₈ O ₄	C ₂₆ H ₃₄ Co ₂ N ₂₈ O ₅	C ₂₆ H ₃₈ N ₂₈ Ni ₂ O ₇	C ₁₆ H ₁₈ CuN ₁₀ O ₂ S ₂
Formula weight	910.68	936.67	972.20	510.06
Crystal system	Triclinic	Triclinic	Triclinic	Monoclinic
Space group	<i>P</i> $\bar{1}$	<i>P</i> $\bar{1}$	<i>P</i> $\bar{1}$	<i>P</i> 2 ₁ / <i>n</i>
<i>a</i> /Å	7.2847(5)	9.0102(5)	8.9684(9)	8.8456(4)
<i>b</i> /Å	11.1996(8)	10.4467(7)	10.6957(17)	23.1159(16)
<i>c</i> /Å	12.3995(9)	12.0381(6)	11.9543(19)	10.5040(4)
α /°	109.220(7)	102.964(5)	103.120(14)	90.00
β /°	102.348(6)	103.733(4)	103.888(14)	98.251(4)
γ /°	100.935(6)	113.575(6)	113.977(13)	90.00
<i>V</i> /Å ³	895.28(11)	941.74(9)	946.6(2)	2125.57(19)
<i>Z</i>	2	1	2	4
<i>D_c</i> /g cm ⁻³	1.689	1.652	1.698	1.594
<i>T</i> /K	106.7	104.1	97.0	105.5
μ /mm ⁻¹	0.786	0.961	1.081	1.261
Reflections collected	5863	6528	5801	8862
Independent reflections	3493	3690	3712	4160
<i>R</i> _{int}	0.0249	0.0303	0.0275	0.0298
<i>GOOF</i>	1.032	1.022	1.057	1.062
<i>R</i> , <i>wR</i> (<i>I</i> > 2σ(<i>I</i>))	0.0370/0.0817	0.0497/0.1198	0.0454/0.1085	0.0453/0.0865
<i>R</i> , <i>wR</i> (all data)	0.0462/0.0869	0.0627/0.1285	0.0532/0.1142	0.0561/0.0915

3 RESULTS AND DISCUSSION

3.1 Crystal structural description

of [Mn₂L₂(N₃)₄(H₂O)₂] (**1**)

X-ray crystal structure determination reveals that complex **1** crystallizes in *P* $\bar{1}$ space group. The complex was characterized by an azide bridged Mn(II) dimer complex, as shown in Fig. 1. In the structure, the two Mn(II) centers are interlinked through two end-to-end bridges. The central Mn(II) adopts a distorted pentagonal seven-coordinated bipyramidal environment. The corresponding bond lengths and bond angles are listed in Table S1. The pentagonal basal plane is constructed by N(1), N(3) and N(5) from the L ligand, N(12) from the EE bridge and O(2) from the coordinated water molecule where the basal cisoid angles (The ideal angle in pentagon is 72°) range from 65.88(6)° to

78.03(7)°. The axial position of Mn(II) in the pentagonal double cone is occupied by N(9) and N(14) from the terminal N₃⁻ and another $\mu_{1,3}$ -azido bridge anion respectively, and its span angle is 175.31(8)°. The axial bond lengths of Mn(1)–N(9) and Mn(1)–N(14) are 2.2114(18) and 2.178(2) Å, respectively. The two $\mu_{1,3}$ -azido bridges are parallel to form a plane, which is characteristic of almost all multinuclear complexes with double EE azide bridges. Due to the bisymmetric $\mu_{1,3}$ -azido bridges, the distance between the two Mn(II) is 5.473(7) Å and the inversion center is at the center of two Mn atoms.

As shown in Fig. 2, the binuclear structure forms a 1D supramolecular structure along the *c*-axis of the crystal through π - π conjugation effect. The dihedral angle is 7.83(9)° and the distance between the centers of mass is 3.639 Å. It can also be seen from Fig. 2 and Table 2 that there are

O(2)–H(2A) \cdots N(12ⁱ) and O(2)–H(2B) \cdots N(9ⁱ) ($i = 1 - x, 2 - y, 1 - z$) weak hydrogen bonds in the crystal lattice of

complex **1**, forming a two-dimensional supramolecular structure.

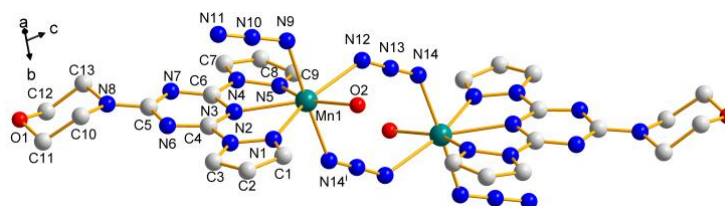


Fig. 1. ORTEP drawing of **1** with atomic number labeling.

Hydrogen atoms have been omitted for clarity. Symmetry code: (i) $1-x, 2-y, 1-z$

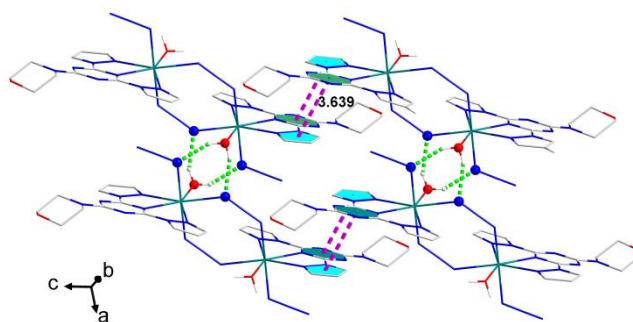


Fig. 2. π - π stacking interactions (pink dashed lines) and intramolecular hydrogen bonds (green dashed lines) in **1**

Table 2. Hydrogen-bond Parameters for **1** (Å, °)

D–H \cdots A	D–H	H \cdots A	D \cdots A	D–H \cdots A
O(2)–H(2A) \cdots N(12 ⁱ)	0.86	2.05	2.855	156
O(2)–H(2B) \cdots N(9 ⁱ)	0.85	2.05	2.815	150

Symmetry code: (i) $1 - x, 2 - y, 1 - z$

3.2 Crystal structural description of [Co₂L₂(N₃)₄](H₂O)₃ (**2**)

Single-crystal X-ray diffraction analysis indicates that complex **2** crystallizes in space group $P\bar{1}$. The labeled diagram for **2** is shown in Fig. 3. The Co²⁺ atoms present identical deformed octahedral environment formed by the L ligand (N(1), N(3), N(5)), a N(9) atom from one bridging azide, a N(9ⁱ) ($i = 1-x, -y, -z$) atom from the symmetry-related bridging azide ligand, and a N(12) atom from the terminal N₃[−]. The L ligand coordinates the Co(II) ion in the equatorial plane through N(1), N(3), N(5) with bond distances (Table S2) similar to those observed in other related compounds^[23]. The nitrogen atom (N(9)) of the azide bridge also participates in the formation of the octahedral basal plane where the basal angles (The ideal angle in quadrilateral is 90°) range from 73.42(10)° to 112.01(11)°. The axial positions of Co(II) in the octahedron are occupied by N(9ⁱ)

and N(12) from the terminal N₃[−] and another EO bridge anion, respectively, and its span angle is 174.18(13)°. The axial bond lengths of Co(1)–N(9ⁱ) and Co(1)–N(12) are 2.186(3) and 2.085(3) Å, respectively. The azide ions are nearly linear with a N(9)–N(10)–N(11) angle of 177.6(4)° and a N(12)–N(13)–N(14) angle of 179.5(5)°. The slightly asymmetric double azide bridges with Co–N(9) bond distances of 2.062(3) and 2.186(3) Å and a Co–N(9)–Co bond angle of 101.24(11)° separate the two Ni(II) ions by 3.285(8) Å, indicating the absence of any bond between them.

As can be seen from Fig. 4, the pyrazolyl and triazine rings from the L ligands of two neighbouring molecules of **2** are basically parallel to each other with a center distance of 3.585 Å and a dihedral angle of 1.741°, showing the existence of significant π - π stacking interactions.

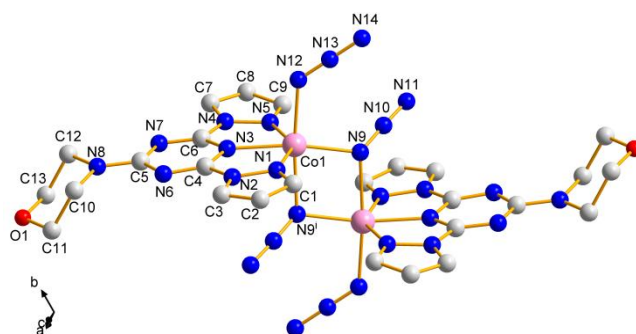


Fig. 3. ORTEP drawing of **2** with the atoms labeling. Hydrogen atoms and solvent molecules have been omitted for clarity. Symmetry code: (i) $1-x, -y, -z$

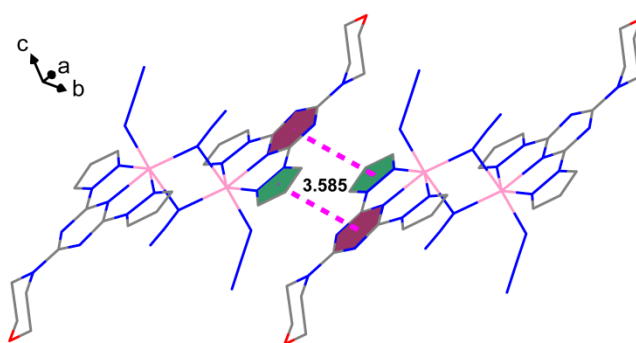


Fig. 4. π - π stacking interactions (pink dashed lines) in **2**. Symmetry code: (i) $1-x, -y, -z$

3.3 Crystal structural description of $[\text{Ni}_2\text{L}_2(\text{N}_3)_3(\text{H}_2\text{O})]\text{N}_3 \cdot (\text{H}_2\text{O})_4$ (**3**)

Complex **3** crystallizes in monoclinic space group $P\bar{1}$. As shown in Fig. 5, the asymmetric unit of complex **3** consists of one Ni^{2+} ion, one L ligand, one $\mu_{1,1}$ -azido bridge anion and a terminal N_3^- . The nickel center is best viewed as a distorted octahedral geometry. The Ni(1) atom is coordinated with three nitrogen atoms (N(1), N(3) and N(5)) from one L ligand, two nitrogen atoms (N(9), N(9ⁱ)) ($i = 2 - x, 2 - y, 1 - z$) from the symmetrical $\mu_{1,1}$ -azido bridges and one nitrogen atom (N(12)) from the terminal N_3^- . The corresponding bond

lengths and bond angles are listed in Table S3. The Ni–N distances fall in the ranges of $1.993(3) \sim 2.195(3)$ Å.

Fig. 6 shows that the pyrazolyl and triazine rings from L ligands of two neighbouring molecules of **3** are basically parallel to each other with a center distance of 3.721 Å and a dihedral angle of 0.482° , showing the existence of significant π - π stacking interactions. In addition, as shown in Fig. 7 and Table 3, there are weak hydrogen bonding interactions in the crystal of **3**. The molecules form a two-dimensional supramolecular structure through π - π conjugate interaction and hydrogen bonding.

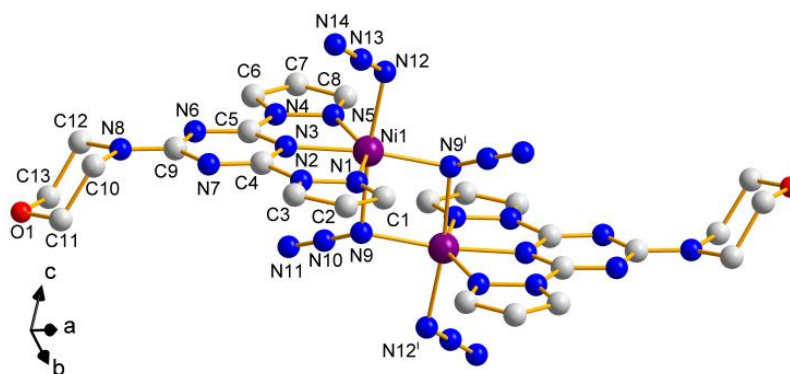


Fig. 5. ORTEP drawing of **3** with atom labeling. Hydrogen atoms and solvent molecules have been omitted for clarity. Symmetry code: (i) $2-x, 2-y, 1-z$

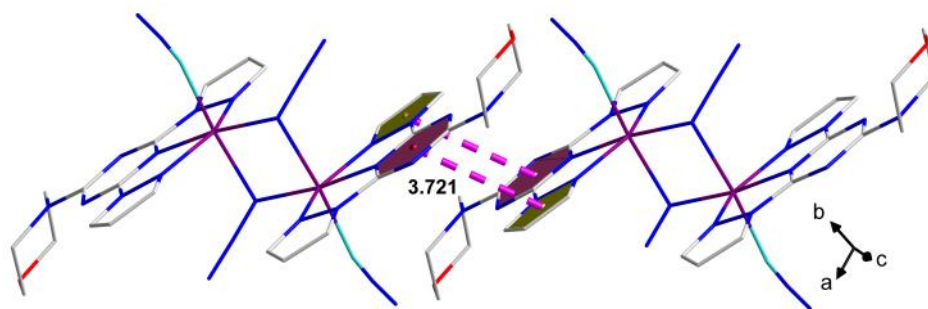


Fig. 6. π - π stacking interactions (pink dashed lines) in **3**. Symmetry code: (i) $2-x, 2-y, 1-z$

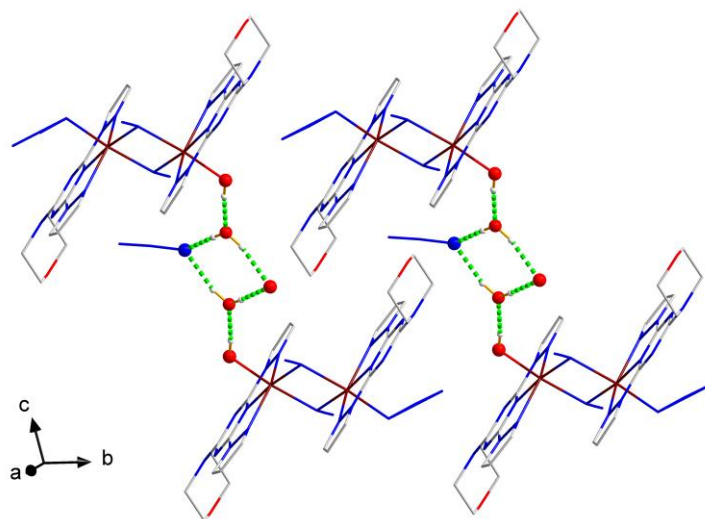


Fig. 7. Intermolecular hydrogen bonds (green dashed lines) in **3**

Table 3. Hydrogen-bond Parameters for **3** (Å, °)

D-H...A	D-H	H...A	D...A	D-H...A
O(2)-H(2A)...O(3 ⁱ)	0.85	1.94	2.787	174
O(3)-H(3A)...N(17)/O(5)	0.86	1.95	2.796	165
O(3 ⁱ)-H(3B ⁱ)...N(17)/O(5 ⁱⁱ)	0.86	1.95	2.805	176

Symmetry codes: (i) $2-x, 1-y, 1-z$; (ii) $1+x, 1+y, 1+z$

3.4 Crystal structural description of [CuL(CH₃OH)(SCN)(NCS)] (**4**)

X-ray diffraction analysis of complex **4** shows that it crystallizes in monoclinic space group $P2_1/n$. As shown in Fig. 8, the copper(II) atom presents a deformed octahedral environment consisting of an L ligand (N(1), N(3), N(5)), an oxygen atom (O(2)) of methanol, a nitrogen atom (N(9)) and a sulfur atom (S(2)) of two thiocyanate anions. Interestingly, the central copper atom was coordinated with a sulfur atom and a nitrogen atom of two thiocyanate ligands, respectively. Selected bond distances and bond angles are listed in Table S4. The L ligand and a thiocyanate ligand coordinate with Cu(II) ion on the equatorial plane through N(1), N(3), N(5) and N(9), and the bond distance range is 1.929(3)~2.415(3) Å. The basal cisoid angle of the octahedral basal plane ranges

from 72.19(10)° to 113.87(10)°. The axial positions of Cu(II) in the octahedron are occupied by S(2) and O(2) from the thiocyanate and coordinated methanol, respectively, and its span angle is 176.29(6)°. The axial bond lengths of Cu(1)-S(2) and Cu(1)-O(2) are 2.4515(8) and 2.117(2) Å. Thiocyanate ions are almost linear, with angles of 179.3(3)° for N(10)-C(15)-S(2) and 179.4(3)° for N(9)-C(14)-S(1).

As can be seen from Fig. 9, the pyrazolyl and triazine rings of the L ligand from two adjacent molecules are parallel to each other, with a center distance of 3.985 Å and a dihedral angle of 8.457°, indicating the significant π - π stacking effect. There is an O(2)-H(2)···N(10) weak hydrogen bond force in the crystal of complex **4**, forming a two-dimensional network structure (Fig. 9 and Table 4).

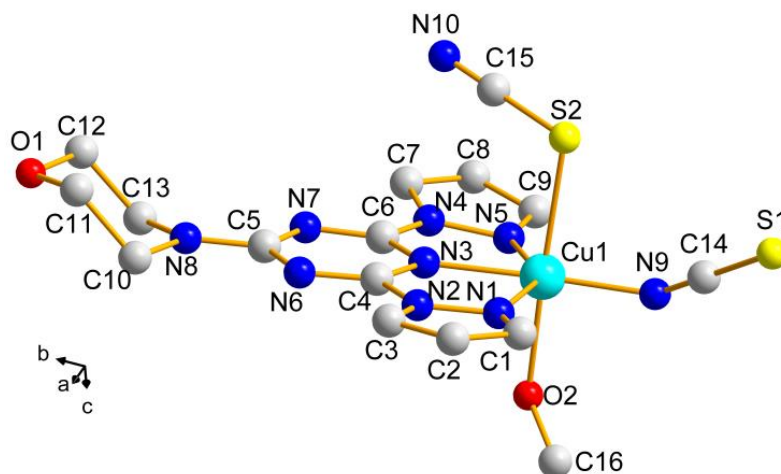


Fig. 8. ORTEP drawing of **4** with atom labeling. Hydrogen atoms have been omitted for clarity

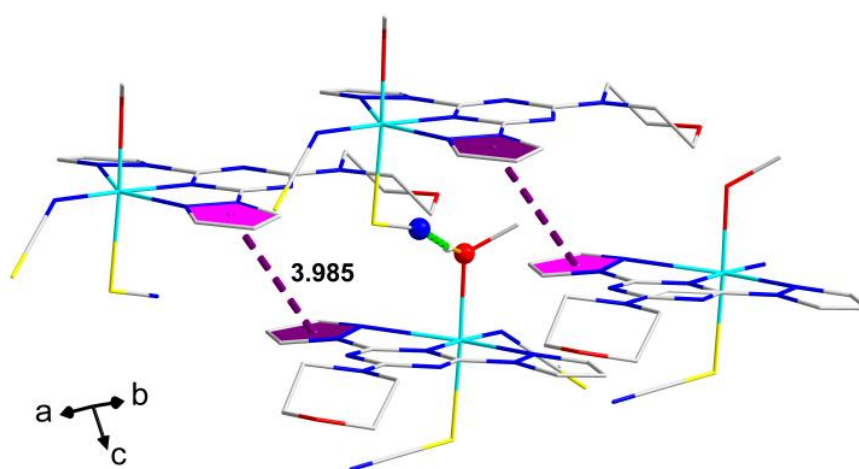


Fig. 9. 2D supramolecular structure with π - π stacking interactions (purple dashed lines) and intermolecular hydrogen bond (green dashed line) in **4**

Table 4. Hydrogen-bond Parameters for **4** (Å, °)

D-H...A	D-H	H...A	D...A	D-H...A
O(2)-H(2)...N(10 ⁱ)	0.85	1.94	2.780	172

Symmetry code: (i) $1/2 + x, 1/2 - y, 1/2 + z$

3.5 Coordination modes of azide and thiocyanate

Azide-crosslinked anions are multifunctional and provide different coordination modes depending on the spatial and electronic requirements of other ligands in the complex. The azide bridging mode is influenced by many factors such as the solvent system, the ratio of metal to ligand, crystallization temperature, the valence state of the central atom and so on^[24-26]. It is worth noting that the azide bridged complexes of the same metal can have different bridged coordination modes. However, no correlation has been found between the properties of the L ligand and the coordination mode of the azide bridge^[27]. In this article, experimental conditions for the preparation of complexes **1**~**3** including raw materials,

experimental temperature and solvents are the same or similar. Interestingly, the bridging methods of azide in the three compounds are different. Among them, the Mn(II) atoms of compound **1** are connected by EE bridges, while the Co(II) and Ni(II) atoms of compounds **2** and **3** are connected by EO bridges. Therefore, the different bridging modes of the three complexes may be attributed to the difference of the central atoms and their coordination environments, in which complex **1** is a seven-coordinated pentagonal bipyramidal structure, while **2** and **3** have octahedral coordination environments around the central metal ion.

In addition, the coordination modes of thiocyanate are various^[28-33]. As we all know, when the thiocyanate ion is the

only ligand in the complex, its bonding method usually follows the hard (M-NCS) or soft (M-SCN) mode throughout the cycle. However, the presence of other ligand also obviously affects whether the thiocyanate ions are bound via N or S bonds. In this work, we successfully synthesized a mononuclear complex of Cu(II) combined with thiocyanate and L ligand. Interestingly, the coordination of the two thiocyanate ions in the complex is different. One nitrogen atom is coordinated and the other is a sulfur atom. In addition, the delicate balance of electronic, space and solvent force also affects the coordination mode of thiocyanate in **4**^[34].

3.6 TG studies

In order to characterize the thermal stability of compounds more comprehensively, TG curves of complexes **1**~**4** were measured in a nitrogen atmosphere with a temperature range of 25~800 °C (Fig. S1). For complex **1**, a weight loss of 4.3% can be observed below 175 °C because of the departure of two coordination water molecules. As the temperature continued to rise, the compound degraded rapidly. The TG curve of complex **2** showed that the weight loss rate was 5.9% before 169 °C due to the removal of three lattice water molecules. With the increase of temperature, the

compound also degraded rapidly. The first weight loss of 8.7% could be observed for complex **3** before 165 °C assigned to the water molecules in the structure. Complex **4** exhibited the first step weight loss of 4.8% below 110 °C owing to the release of coordinated methanol molecule. When higher than 260 °C, it decomposed rapidly.

3.7 Fluorescence properties

Considering that the four complexes are composed of π -conjugated ligands and *d*-electron metal centers, we speculate that they may be fluorescent materials. Therefore, the emission spectra of the free ligand L and the four complexes were recorded in solution at room temperature. As shown in Fig. 10, the L ligand and the four complexes exhibited an emission band of λ_{max} about 412 nm when excited at 258 nm. The order of fluorescence emission intensity from high to low is $L > 3 > 2 > 4 > 1$. The fluorescence emission peak has a wavelength range of 350 to 500 nm. The emissions of complexes **1**~**4** can be attributed to intra-ligand $\pi \rightarrow \pi^*$ transitions of L, not to MLCT (metal-to-ligand charge transfer) or LMCT (ligand-to-metal charge transfer).

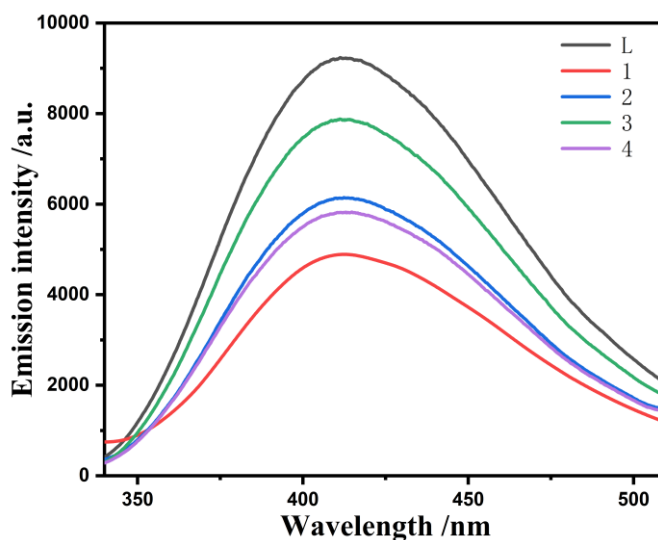


Fig. 10. Fluorescence spectra of L ligand and complexes **1**~**4**

4 CONCLUSION

The azide bridged complexes of Mn(II), Co(II) and Ni(II) were prepared in the similar experimental conditions and their structures were characterized. Interestingly, the bridging modes of the three compounds are different. Among them, the Mn(II) atoms of compound **1** are connected by the EE bridge, while the Co(II) and Ni(II) atoms of compounds **2** and

3 are connected by the EO bridge. In addition, the mononuclear complex **4** of Cu(II) combined with thiocyanate and L ligand was successfully synthesized and the coordination of the two thiocyanate ions in **4** is different. Additionally, π - π stacking interactions and hydrogen bonds were observed in the structures of **1**~**4** and the TG and fluorescence properties of them were studied.

REFERENCES

- (1) Luo, T. F.; Ji, X. F.; Zhu, C. Y. Synthesis, crystal structures, and anti-cervical cancer activity evaluation of three trinuclear transition metal(II) complexes with N,O-donor schiff base ligand. *Z. Anorg. Allg. Chem.* **2019**, 45, 777–785.
- (2) Ge, Z. J.; Shehzad, M. A.; Ge, L.; Zhu, Y.; Wang, H. J.; Li, G.; Zhang, J. J.; Ge, X. L.; Wu, L.; Xu, T. W. Beneficial use of a coordination complex as the junction catalyst in a bipolar membrane. *ACS Appl. Energy Mater.* **2020**, 3, 5765–5773.
- (3) Hanafi, S.; Trache, D.; He, W.; Xie, W. X.; Mezroua, A.; Yan, Q. L. Thermostable energetic coordination polymers based on functionalized GO and their catalytic effects on the decomposition of AP and RDX. *J. Phys. Chem. C* **2020**, 124, 5182–5195.
- (4) Mandal, S.; Nanavati, S. P.; Willock, D. J.; Ananthakrishnan, R. Photoactive Ag(I)-based coordination polymer as a potential semiconductor for photocatalytic water splitting and environmental remediation: experimental and theoretical approach. *J. Phys. Chem. C* **2019**, 123, 23940–23950.
- (5) Benaissa, H.; Wolff, M.; Robeyns, K.; Knör, G.; Hecke, K. V.; Campagnol, N.; Franssaer, J.; Garcia, Y. Syntheses, crystal structures, luminescent properties, and electrochemical synthesis of group 12 element coordination polymers with 4-substituted 1,2,4-triazole ligands. *Cryst. Growth Des.* **2019**, 19, 5292–5307.
- (6) Song, X. Q.; Meng, H. H.; Lin, Z. G.; Wang, L. 2D lanthanide coordination polymers: synthesis, structure, luminescent properties, and ratiometric sensing application in the hydrostable PMMA-doped hybrid films. *ACS Appl. Polym. Mater.* **2020**, 2, 1644–1655.
- (7) Feng, X.; Chen, J. L.; Bai, R. F.; Wang, L. Y.; Wei, J. T.; Chen, X. X. Two unique cobalt-organic frameworks based on substituted imidazole-dicarboxylate and dipyriddy-type ancillary ligands: crystal structures and magnetic properties. *Inorg. Chem. Commun.* **2016**, 66, 41–46.
- (8) Sun, G. C.; Yu, L. L.; Hu, Y.; Sha, Y. Y.; Rong, H. R.; Li, B. L.; Liu, H. J.; Liu, Q. A manganese-based coordination polymer containing no solvent as a high performance anode in Li-ion batteries. *Cryst. Growth Des.* **2019**, 19, 6503–6510.
- (9) Amores, M.; Wada, K.; Sakaushi, K.; Nishihara, H. Reversible energy storage in layered copper-based coordination polymers: unveiling the influence of the ligand's functional group on their electrochemical properties. *J. Phys. Chem. C* **2020**, 124, 9215–9224.
- (10) Dong, S. Y.; Zheng, Q.; Huang, G. Q.; Wang, X. H.; Huang, T. L. The coordination polymer [Cu(bipy)(SO₄)]_n and its functionalization for selective removal of two types of organic pollutants. *Ind. Eng. Chem. Res.* **2019**, 58, 15416–15424.
- (11) Li, W.; Jiang, H. X.; Geng, Y.; Wang, X. H.; Gao, R. Z.; Tang, A. N.; Kong, D. M. Facile removal of phytochromes and efficient recovery of pesticides using heteropore covalent organic framework-based magnetic nanospheres and electrospun films. *ACS Appl. Mater. Interfaces.* **2020**, 12, 20922–20932.
- (12) Liang, C. J.; Ren, J. H.; Hankari, S. E.; Huo, J. Aqueous synthesis of a mesoporous Zr-based coordination polymer for removal of organic dyes. *ACS Omega.* **2020**, 5, 603–609.
- (13) Ma, J. C.; Tang, Y. X.; Cheng, G. B.; Imler, G. H.; Parrish, D. A.; Shreeve, J. M. Energetic derivatives of 8-nitropyrzolo[1,5-a][1,3,5]triazine-2,4,7-triamine: achieving balanced explosives by fusing pyrazole with triazine. *Org. Lett.* **2020**, 22, 1321–1325.
- (14) Berdiell, I. C.; Kulmaczewski, R.; Halcrow, M. A. Iron(II) complexes of 2,4-dipyrazolyl-1,3,5-triazine derivatives-the influence of ligand geometry on metal ion spin state. *Inorg. Chem.* **2017**, 56, 8817–8828.
- (15) Berdiell, I. C.; Kulak, A. N.; Warriner, S. L.; Halcrow, M. A. Heterometallic coordination polymer gels supported by 2,4,6-tris(pyrazol-1-yl)-1,3,5-triazine. *ACS Omega* **2018**, 3, 18466–18474.
- (16) Biswas, R.; Mukherjee, S.; Kar, P.; Ghosh, A. A rare phenoxido/acetato/azido bridged trinuclear and an unprecedented phenoxido/azido bridged one-dimensional polynuclear nickel(II) complexes: synthesis, crystal structure, and magnetic properties with theoretical investigations on the exchange mechanism. *Inorg. Chem.* **2012**, 51, 8150–8160.
- (17) Chu, J. F.; Zhang, M. Y.; Wang, Y. Q. Syntheses, crystal structures, and properties of three copper(II) complexes constructed by 4-(4,6-bis(1H-pyrazol-1-yl)-1,3,5-triazin-2-yl)morpholine. *Z. Anorg. Allg. Chem.* **2017**, 643, 1101–1106.
- (18) Chen, W.; Chu, J. F.; Wang, Y. Q. Synthesis, characterization and preliminary reactivity behaviors with transitional metals of a new polydentate N-donor ligand. *J. Mol. Struct.* **2014**, 1068, 237–244.
- (19) Chu, J. F.; Wang, S. Y.; Zhang, M. Y.; Xu, Q. X.; Wang, Y. Q. Syntheses, crystal structures, non-covalent interactions and properties of a nickel(II) complex monomer and its dimer. *Chin. J. Struct. Chem.* **2020**, 39, 1877–1984.
- (20) Dolomanov, O. V.; Bourhis, L. J.; Gildea, R. J.; Howard, J. A. K.; Puschmann, H. OLEX2: a complete structure solution, refinement and analysis program. *J. Appl. Cryst.* **2009**, 42, 339–341.
- (21) Sheldrick, G. M. A short history of SHELX. *Acta Crystallogr. Sect. A* **2008**, 64, 112–122.
- (22) Sheldrick, G. M. SHELXT – integrated space-group and crystal-structure determination. *Acta Crystallogr. Sect. C* **2015**, 71, 3–8.

- (23) Boonmak, J.; Nakano, M.; Chaichit, N.; Pakawatchai, C.; Youngme, S. Spin canting and metamagnetism in 2D and 3D cobalt(II) coordination networks with alternating double end-on and double end-to-end azido bridges. *Inorg. Chem.* **2011**, 50, 7324–7333.
- (24) Yue, Y. F.; Gao, E. Q.; Fang, C. J.; Zheng, T.; Liang, J.; Yan, C. H. Three azido-bridged Mn(II) complexes based on open-chain diazine Schiff-base ligands: crystal structures and magnetic properties. *Cryst. Growth Des.* **2008**, 8, 3295–3301.
- (25) Das, A.; Rosair, G. M.; Fallah, S. E.; Ribas, J.; Mitra, S. Weak metamagnetic-like 1D manganese(II) complex with a double $\mu_{1,1}$ -azido bridge: a structure and magnetic study. *Inorg. Chem.* **2006**, 45, 3301–3306.
- (26) Dey, S. K.; Mondal, N.; Fallah, M. S. E.; Vicente, R.; Escuer, A.; Solans, X.; Font-Bard, M.; Matsushita, T.; Gramlich, V.; Mitra, S. Crystal structure and magnetic interactions in nickel(II) dibridged complexes formed by two azide groups or by both phenolate oxygen-azide, -thiocyanate, -carboxylate, or -cyanate groups. *Inorg. Chem.* **2004**, 43, 2427–2434.
- (27) Bhat, S. A.; Palakurthy, N. B.; Kambhala, N.; Subramanian, A.; Rao, D. S. S.; Prasad, S. K.; Yelamaggad, C. V. Gram-scale synthesis and multifunctional properties of a two-dimensional layered copper(II) coordination polymer. *ACS Appl. Polym. Mater.* **2020**, 2, 1543–1552.
- (28) Zhang, H.; Wang, X.; Zhu, H.; Xiao, W.; Zhang, K.; Teo, B. K. Anisotropic templating effect in the formation of two-dimensional anionic cadmium-thiocyanate coordination solids $[(12C4)_2Cd][Cd_2(SCN)_6]$ and $[(12C4)_2Cd][Cd_3(SCN)_8]$ with checkerboard and herringbone patterns, respectively. *Inorg. Chem.* **1999**, 38, 886–892.
- (29) Brooker, S.; Plieger, P. G.; Moubaraki, B.; Murray, K. S. $[Co^{II}_2L(NCS)_2(SCN)_2]$: the first cobalt complex to exhibit both exchange coupling and spin crossover effects. *Angew. Chem. Int. Ed.* **1999**, 38, 408–410.
- (30) Bai, Y.; Hu, X. F.; Dang, D. B.; Bi, F. L.; Niu, J. Y. Synthesis, crystal structure and luminescent properties of one new inorganic-organic hybrid compound $[O_2NBzQL]_4[Cd(SCN)_4(NCS)_2]$ ($O_2NBzQL = 1-(4'-NO_2\text{-benzyl})\text{quinolinium cation}$). *Spectrochim Acta A Mol Biomol Spectrosc.* **2011**, 78, 70–73.
- (31) Chiumia, G. C.; Craig, D. C.; Phillips, D. J.; Rae, A. D.; Kaifi, F. M. Z. Terminal *s*-coordinated thiocyanate in a nickel(II) complex. X-ray structures of $Ni(poph)(H_2O)(SCN)(NCS)$ and $Ni(poqh)(H_2O)(NCS)_2$ ($poph = 2\text{-pyridinecarboxaldehyde 1-oxide 2'-pyridinyl-hydrazone}$, $poqh = 2\text{-pyridinecarboxaldehyde 1-oxide 2'-quinolynyl-hydrazone}$). *Inorg. Chim. Acta* **1999**, 285, 297–300.
- (32) Kishi, S.; Kato, M. Thermal and photo control of the linkage isomerism of bis(thiocyanato)(2,2'-bipyridine)platinum(II). *Inorg. Chem.* **2003**, 42, 8728–8734.
- (33) Wang, Z.; Liu, T.; Long, X.; Li, Y.; Bai, F.; Yang, S. Understanding the diverse coordination modes of thiocyanate anion on solid surfaces. *J. Phys. Chem. C* **2019**, 123, 9282–9291.
- (34) Meek, D. W.; Nicpon, P. E.; Meek, V. I. Mixed thiocyanate bonding in palladium(II) complexes of bidentate ligands. *J. Am. Chem. Soc.* **1970**, 92, 5351–5359.